

## Pinning Frequencies of the Collective Modes in $\alpha$ -Uranium

B. Mihaila, C. P. Opeil, F. R. Drymiotis, J. L. Smith, J. C. Cooley, M. E. Manley, A. Migliori, C. Mielke, T. Lookman, A. Saxena, A. R. Bishop, K. B. Blagoev, D. J. Thoma, and J. C. Lashley  
*Los Alamos National Laboratory, Los Alamos, New Mexico 87545, USA*

B. E. Lang, J. Boerio-Goates, and B. F. Woodfield  
*Department of Chemistry and Biochemistry, Brigham Young University, Provo, Utah 84602, USA*

G. M. Schmiedeshoff  
*Department of Physics, Occidental College, Los Angeles, California 90041, USA*  
(Received 26 July 2005; published 21 February 2006)

Uranium is the only known element that features a charge-density wave (CDW) and superconductivity. We report a comparison of the specific heat of single-crystal and polycrystalline  $\alpha$ -uranium. In the single crystal we find excess contributions to the heat capacity at 41 K, 38 K, and 23 K, with a Debye temperature  $\Theta_D = 256$  K. In the polycrystalline sample the heat capacity curve is thermally broadened ( $\Theta_D = 184$  K), but no excess heat capacity was observed. The excess heat capacity  $C_\phi$  (taken as the difference between the single-crystal and polycrystal heat capacities) is well described in terms of collective-mode excitations above their respective pinning frequencies. This attribution is represented by a modified Debye spectrum with two cutoff frequencies, a pinning frequency  $\nu_0$  for the pinned CDW (due to grain boundaries in the polycrystal), and a normal Debye acoustic frequency occurring in the single crystal.

DOI: [10.1103/PhysRevLett.96.076401](https://doi.org/10.1103/PhysRevLett.96.076401)

PACS numbers: 71.45.Lr, 05.70.Fh, 05.70.Jk

New ground states and modulated structures arise in low-dimensional solids [1], but are of particular interest when they occur in solids that are not low-dimensional, such as  $\alpha$ -uranium ( $\alpha$ -U) [2]. When periodic, these ordered structures may be a spin-density wave (SDW) as found in chromium [3] or a charge-density wave (CDW) as found in metal dichalcogenides [4] and in  $\alpha$ -U [5]. Uranium is unique in the periodic table in that it is the *only* element known to exhibit a CDW in the absence of distortions due to a SDW. Although detailed band-structure calculations on the CDW transitions have been carried out [6], knowledge of the CDW energetics in  $\alpha$ -U remains to be experimentally verified.

Across the light actinide elements (thorium—plutonium) itinerant  $5f$ -electrons lower their energies by causing Peierls-like distortions [7], leading to the lowest-symmetry structures in the periodic table. Like their quasi-one- and two-dimensional counterparts, the collective mode in the crystal is characterized by an energy gap in the single-particle excitation spectrum originating from a charge modulation of the periodic lattice [8],  $\rho(x) = \rho_0 + \Delta\rho \cos(2k_F x + \phi)$ , where  $\rho_0$  is the density of the normal state,  $\Delta\rho$  is the amplitude of the CDW,  $k_F$  is the Fermi wave vector, and  $\phi$  is a phase factor defining the position of the periodic modulation.

In a perfect lattice, a CDW should be able to slide throughout the crystal without resistance like a superconductor, as suggested by Fröhlich [9]. However, in real crystals pinning by disorder from microstructure (defects, twins, grain boundaries, impurities, surfaces, etc.) elevates the collective mode to finite frequencies expressed by a threshold electric field,  $E_{th}$ . The threshold field is

usefully characterized within a single-particle model [4]. In this model, the collective mode is described by the equation of motion of a classical particle moving in a periodic potential. If a small dc field is applied near the threshold field, the particle may be displaced from the bottom of the well. For fields less than  $E_{th}$  the particle remains localized within the potential. For electric fields greater than  $E_{th}$  the particle slides down the potential leading to an extra contribution to the conductivity generated by motion of the collective mode through the crystal, or Fröhlich conduction.

Significant differences in single and polycrystalline uranium have been observed in the thermal expansion, high temperature neutron diffraction, and calorimetry [10,11]. The temperature dependence of the thermal expansion coefficients for single-crystal uranium differ in the three orthorhombic principle directions [5]. Presumably a simple ensemble average for a polycrystal sample would display a temperature dependence different from any in the single crystal. Therefore it was anticipated that a comparison of the single-crystalline and polycrystalline specific heat would provide a useful probe of the effects on the Debye spectrum associated with microstructural effects. In this Letter we show that the differences between the specific heat of crystals that undergo the weakly pinned CDW transitions (single crystals) and those that are strongly pinned CDW (polycrystals) provide a definitive way to determine the energetics of pinning.

Biljakovic *et al.* [12] have described the effect of collective-mode dynamics on the phonon spectrum. In these cases, a CDW modifies the phonon spectrum, which can be described by a mixture of acoustic and optic modes.

The modified Debye spectrum features two cutoff frequencies: a lower frequency corresponding to a pinned state,  $h\nu_0 = k_B T_0$ , and an upper frequency,  $h\nu_\phi = k_B \Theta_\phi$ , corresponding to the normal Debye temperature for the collective modes [12]. With this modification, the excess heat capacity  $C_\phi$  (i.e., the difference between the specific heats of the single- and polycrystal,  $C_\phi = C_{\text{single}} - C_{\text{poly}}$ ) can be written as [13]

$$C_\phi^{\text{fit}} = 3N_\phi k_B \left( \frac{T}{\Theta_\phi} \right)^3 \int_{T_0/T}^{\Theta_\phi/T} dx (x - x_0)^2 \frac{x^2 e^x}{(e^x - 1)^2}, \quad (1)$$

where we have introduced the notation  $x = h\nu/(k_B T)$  with  $k_B$  being the Boltzmann constant, and  $N_\phi$  denotes the number of excitations involved in the transition.

Single crystals of uranium were formed from electrotransport in a molten LiCl-KCl eutectic electrolyte containing  $\text{UCl}_3$  at approximately 3 wt %, as described elsewhere [14]. After the single crystals were measured, they were cast through induction melting of the single crystals in a BeO crucible, under an inert atmosphere, to prepare polycrystalline samples of the same pedigree. The sample was melted only once to minimize the possibility of contamination from the crucible or the carrier gas, then cleaned in concentrated nitric acid. The grain sizes were 20–50  $\mu\text{m}$ . The low-temperature specific heat of the samples were measured using a semiadiabatic calorimeter [15] in the temperature range  $\sim 0.5$  to 100 K. The single crystal had a mass of 0.5 g and the polycrystalline sample mass was 1.4 g.

The effect of microstructure on collective-mode pinning is shown in Fig. 1. The  $C/T$  versus  $T$  curves for polycrystal uranium and single crystal show a different contribution throughout the temperature range encompassing the CDW state. Specifically, three CDW transitions are observed in the single crystal at 23 K ( $\alpha_3$ ), 38 K ( $\alpha_2$ ), and 41 K ( $\alpha_1$ ). While the polycrystalline sample shows no sharp excess heat capacity in Fig. 1, one sees a significant difference in the single-crystal sample. Starting below the  $\alpha_3$  transition, the heat capacity of the polycrystalline sample is larger. The heat capacity is lower at the  $\alpha_3$  transition returning to a larger value upon warming to temperatures between the  $\alpha_3$  and  $\alpha_2$  transitions. Similarly it returns to a lower value through  $\alpha_2$  and  $\alpha_1$  transitions. This excess at the transitions is shown in the excess entropy,  $\Delta S_\phi = S_{\text{single}} - S_{\text{poly}}$ , depicted in the inset of Fig. 1(a). The excess contributions are consistent with the formation of an energy gap in the single crystal that is much larger than that observed in the polycrystal. Above the CDW transitions the difference in entropy has been determined through neutron diffraction and calorimetric measurements of Manley and co-workers to arise from a microstrain contribution at the grain boundary interfaces in polycrystalline uranium [11].

As with familiar 1D and 2D CDWs, we anticipate that the CDW transitions correspond to a lock-in commensurate with the periodicity of the underlying lattice, separated by mixed phases of commensurate spatial regions and

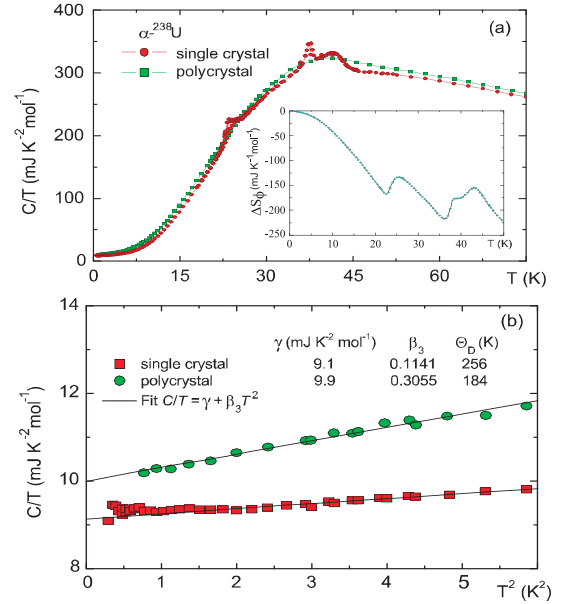


FIG. 1 (color). Measured specific heat plotted as  $C/T$  vs  $T$ . The transitions at 38 and 41 K are broadened in the polycrystal, as the specific heat for the polycrystal rises more quickly before the onset of the transition in the single crystal. The inset shows the temperature dependence of the excess entropy  $\Delta S_\phi = S_{\text{single}} - S_{\text{poly}}$ .

discommensurations [16]. Phonon softening in  $\alpha$ -U has been observed below 50 K [17]. The new unit cell doubles in the [100] direction ( $a$  direction) at  $T_{\alpha_1} = 41$  K, becomes 6 times larger in the [010] direction ( $b$  direction) at  $T_{\alpha_2} = 38$  K, and becomes nearly 6 times larger in the [001] direction with the same periodicity (commensurate) along the  $b$  direction, at  $T_{\alpha_3} = 23$  K [5]. Consequently, the volume of the new cell is 6000  $\text{\AA}^3$ . Pinning of the collective modes by microstructure, also consistent with thermal expansion measurements, results in the polycrystal exhibiting a minimum in  $(\Delta L/L)$  between 45 and 50 K. The relative volume change between 4 and 50 K is significantly larger in single crystals [5,10].

Further evidence for the collective-mode pinning is provided by the linear region of the low-temperature specific heat [see Fig. 1(b)], where we notice a pronounced difference in the low-temperature Debye limit. Figure 1(b) shows an expanded view of  $C/T$  vs  $T^2$ . Below 10 K, each data set was fit to the electronic and lattice specific heat

$$C/T = \gamma + \beta_3 T^2. \quad (2)$$

The Debye temperature  $\Theta_D$  was obtained from  $\beta_3$ , as

$$\Theta_D = \sqrt[3]{12\pi^4 R/5\beta_3}, \quad (3)$$

while the  $y$  intercept gives the electronic specific heat,  $\gamma$ . The parameters obtained from the fit to Eq. (2), and the inferred Debye temperatures are listed in Fig. 1(b). The most striking difference between the two samples is that the slope,  $\beta_3$ , increases by a factor of 3 in the polycrystalline sample, resulting in a 35% reduction in  $\Theta_D$  [18].

The large differences in the specific heat of the single-crystal and polycrystalline samples between 15 K and 60 K [Fig. 1(a)] and the low-temperature limiting Debye temperatures [Fig. 1(b)] suggest a modified Debye spectrum, as in Eq. (1). The excess heat capacity  $C_\phi$  as a function of temperature is depicted in Fig. 2. In other words,  $C_\phi$  represents the heat capacity of the collective modes above their respective pinning frequencies. Anomalies such as these are known to arise from the phonon-branch splitting into an optic mode and an acoustic mode below the CDW condensate formation. Such features cannot be reproduced from a normal Debye model or Debye-Einstein models, and in order to analyze the three anomalies, it is necessary to consider the two different Debye temperatures obtained in Eq. (3) and to fit the excess specific heat  $C_\phi$  using the integral evaluated at temperatures near the transitions. This description of the modified Debye spectrum is further evident from the fact that  $\Theta_D$  obtained from the single crystal is the only calorimetric value [15] to match the value obtained from elastic constant measurements [20].

Keeping  $N_\phi$  and  $\nu_0$  as free parameters, and  $\Theta_\phi$  fixed to the single-crystal value listed in Fig. 1(b), the low-temperature fit for the polycrystalline sample leads to the following  $N_\phi/N_A$  values: 0.25 for  $\alpha_1$ , 0.55 for  $\alpha_2$ , and 0.9 for  $\alpha_3$  ( $N_A$  is the Avogadro number). The values obtained for the pinning frequencies are indicated in Fig. 2 for each transition [21]. These values are consistent with electronic structure calculations [6], but pinning to microstructure at  $\alpha_1$  occurs by the opening of two gaps in the Fermi surface, accompanied by a doubling of the unit cell in the  $a$  direction. In essence, the two areas of the Fermi surface with the highest density of states are nested in the  $a$  direction. Because there are two energy scales involved in this transition (the lattice distortion energy and the electronic energy) and because there is a nesting in the  $b$  direction only 2 K lower than the  $\alpha_1$  transition, it is apparent that the  $\alpha_2$  transition is necessary to overcome the overall lattice distortion energy: the doubling of the unit cell in the  $a$  direction at 41 K leaves the Fermi surface in a favorable

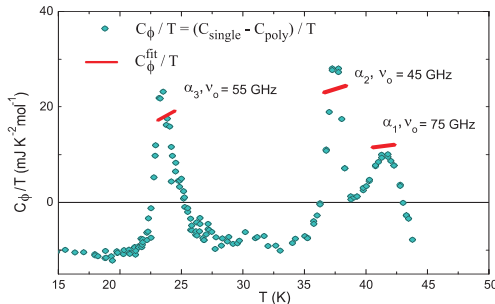


FIG. 2 (color). Excess specific heat plotted as  $C_\phi/T$  vs  $T$ . Note the excess specific heat can be negative since we neglected the pinning of the collective mode in the single crystal. The lines depict  $C_\phi^{\text{fit}}/T$  in the peak region, where  $C_\phi^{\text{fit}}$  is calculated from the modified Debye law, Eq. (1), with the individual pinning frequencies shown above each transition.

geometry for nesting in the  $b$  direction, which is possible because there is elastic energy available to further lower the electronic energy [see inset in Fig. 1(a)].

The estimated values of the pinning frequency are lower than those obtained for  $\text{NbTe}_4$  (540 GHz) and  $\text{KCP}$  (200 GHz) but similar to  $(\text{TaSe}_4)_2\text{I}$  (42 GHz), where non-linear conduction due to CDW motion is observed [22]. From the pinning frequencies, we estimate a lower bound on the threshold electric field [8], as

$$E_{\text{th}} = \frac{1}{2} m^* \omega_0^2 / e k_F, \quad (4)$$

where  $m^*$  is the effective mass and  $\nu_0 = \omega_0/(2\pi)$  is the pinning frequency obtained from the fit of the excess specific heat capacity to Eq. (1). With  $m^* k_F = 16.6 \times 10^{-30} \text{ eVs}^2/\text{atom}$ , one obtains  $E_{\text{th}}$  as 14.5, 89, and 133 V/cm for the  $\alpha_1$ ,  $\alpha_2$ , and  $\alpha_3$  transitions, respectively. Here, we have approximated the period ( $\pi/k_F$ ) of the CDW, by  $2a$  in the case of the  $\alpha_1$  transition, and  $4b$  in the case of the  $\alpha_2$  and  $\alpha_3$  transitions.

In light of the above discussion, we suggest that the solution of the long-standing discrepancies in  $\alpha$ -U between the Debye temperatures obtained from calorimetry and elastic constant measurements depends on the degree of pinning of the collective mode. It is interesting to compare these energies for  $\alpha$ -U with other well-known CDW materials; see Fig. 3. At the lowest energy,  $\text{NbSe}_3$  represents the most widely studied CDW material [23]. Here, the single-particle energy gap was studied as a function of defect concentration by subjecting the samples to radiation damage. The threshold field increases linearly with defect concentration supporting strong pinning similar to  $\text{TaSe}_3$  [24] and  $\text{K}_{0.3}\text{MnO}_3$  [23]. In  $\alpha$ -U the CDW state melts at  $T = 41 \text{ K}$  ( $\alpha_1$ ) giving a frequency of 75 GHz for the collective mode. Here the doubling of the unit cell in the  $a$  direction cuts the Brillouin zone in half forming a gap with energy 14.5 V/cm. Similarly, the  $\alpha_2$  transition occurs by nesting of the Fermi surface with less density of states in the  $b$  direction. At  $\alpha_3$  the collective mode is confined to the bottom of the well. Hence, the pinning frequency and the threshold electric field are higher.

The confinement of the collective modes to GHz frequencies in  $\alpha$ -U is a result of topological defects combined with low transformation temperatures. This effect is clear in the  $\alpha_3$  transition where sluggish kinetics are observed, as shown in Fig. 4. Upon slow cooling from the incommensurate state (35 K) to 20 K, and then measuring on

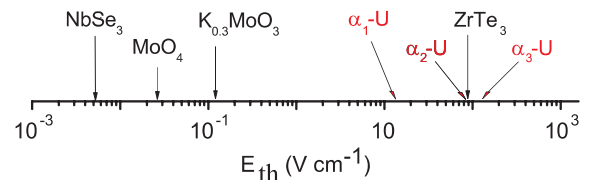


FIG. 3 (color). Estimated electric field threshold energies for  $\alpha_1$  and  $\alpha_2$  transitions in  $\alpha$ -U shown with some common quasi- and two-dimensional CDW systems.

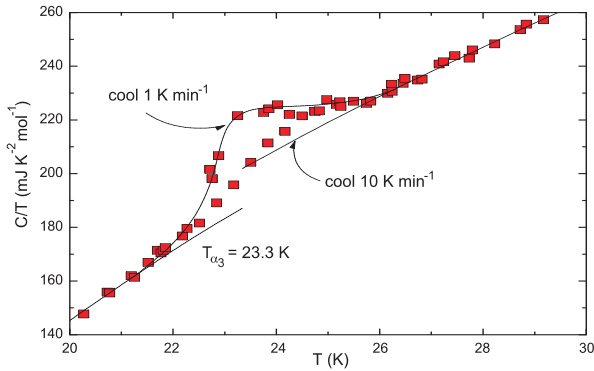


FIG. 4 (color). Dependence of the commensurate CDW transition with cooling time. The transition is apparent only if the sample has been cooled slowly ( $1 \text{ K min}^{-1}$ ). With faster cooling the  $\alpha_3$  transition is no longer resolved, blending in with the background.

warming, the transition appears as a symmetric bump. In contrast, when the sample is cooled 10 times faster, the transition is not detected. Hysteretic effects are known to be more pronounced with decreasing temperatures. As pointed out by Grüner for nonlinear I-V measurements in  $\text{NbSe}_3$ , the high temperature onset is accompanied by oscillatory phenomena and evolves into a hysteresis behavior at low temperature [25]. This behavior has been attributed to extended pinning centers or topological defects [26].

In summary, we have measured the specific heat difference between single-crystal and polycrystalline  $\alpha$ -U and have described the excess heat capacity as the contribution of the collective modes above their respective pinning frequencies. Below the CDW melting temperature of 41 K, the phonon splits into a mixture of acousticlike and opticlike phonon modes as evidenced by the difference in Debye temperatures, 256 K for the single crystal and 184 K for the polycrystal. The long-standing discrepancy between Debye temperatures obtained by calorimetry and elastic constants can be attributed to the degree of pinning of the collective mode. The commensurate transition at 23 K exhibits sluggish kinetics, likely due to topological defects present at low temperatures. Similar collective phenomena are likely to exist in other actinides. Recently, a Kohn-like anomaly [27] in the  $\text{TA}_1$  [011] branch, with softening of the [111] transverse modes, has been observed in the vibrational spectrum of fcc-stabilized plutonium [28,29], and the formation of the  $\alpha'$ -martensite lattice instability has been detected in the low-temperature specific heat [30].

This work was carried out under the auspices of the U.S. Department of Energy. The authors thank P.S. Riseborough, G.H. Lander, and M.F. Hundley for useful discussions.

- [1] R.E. Peierls, *Quantum Theory of Solids* (Oxford University Press, New York, 1955).
- [2] Initially proposed by M.L. Boriack and A.W. Overhauser, *Phys. Rev. B* **18**, 6454 (1978).
- [3] R. Pynn, W. Press, S.M. Shapiro, and S.A. Werner, *Phys. Rev. B* **13**, 295 (1976).
- [4] G. Grüner and A. Zettl, *Phys. Rep.* **119**, 117 (1985).
- [5] G.H. Lander, E.S. Fisher, and S.D. Bader, *Adv. Phys.* **43**, 1 (1994).
- [6] L. Fast *et al.*, *Phys. Rev. Lett.* **81**, 2978 (1998).
- [7] Below the transition thermally activated carriers remain so that no complete Peierls insulating state is formed.
- [8] G. Grüner, *Rev. Mod. Phys.* **60**, 1129 (1988).
- [9] H. Fröhlich, *Proc. R. Soc. A* **223**, 296 (1954).
- [10] J.C. Jousset, *Acta Metall.* **14**, 193 (1966).
- [11] M.E. Manley *et al.*, *Phys. Rev. B* **66**, 024117 (2002).
- [12] K. Biljakovic *et al.*, *Phys. Rev. Lett.* **57**, 1907 (1986).
- [13] In applying Eq. (1) to transition metal chalcogenides [12] the excess specific heat,  $C_\phi$ , was defined as the difference between the specific heat of the sample and the Debye specific heat.
- [14] C.C. McPheeters, E.C. Gay, P.J. Karell, and J. Ackerman, *JOM* **49**, 22 (1997).
- [15] J.C. Lashley *et al.*, *Phys. Rev. B* **63**, 224510 (2001).
- [16] P. Bak and V.J. Emery, *Phys. Rev. Lett.* **36**, 978 (1976).
- [17] H.G. Smith and G.H. Lander, *Phys. Rev. B* **30**, 5407 (1984).
- [18] Using the band structure  $\gamma_{\text{bs}} = 5.89 \text{ mJ K}^2 \text{ mol}^{-1}$  [19], the electron-phonon parameter  $\lambda = \gamma_{\text{bs}}/\gamma^{-1}$  is determined to be 0.5 for the single-crystal, and 0.7 for the polycrystalline sample.
- [19] Band-structure calculations for  $\alpha$ -U were performed using an augmented-plane-wave method with added local orbitals (P. Blaha *et al.*, *WIEN2K, An Augmented Plane Wave Plus Local Orbitals Program for Calculating Crystal Properties* (Technische Universität, Wien, Austria, 2001), for the experimental lattice parameters  $a = 2.858 \text{ \AA}$ ,  $b = 5.876 \text{ \AA}$ ,  $c = 4.955 \text{ \AA}$ .
- [20] E.S. Fisher and H.J. McSkimin, *J. Appl. Phys.* **29**, 1473 (1958).
- [21] Dynamic measurements of the pinning frequencies  $\nu_0$  and of the number of excitations  $N_\phi$  are necessary to validate the values quoted here.
- [22] S. Mori *et al.*, *Physica (Amsterdam)* **329–333B**, 1298 (2003).
- [23] W.W. Fuller, G. Grüner, P.M. Chaikin, and N.P. Ong, *Phys. Rev. B* **23**, 6259 (1981).
- [24] G. Mihály and L. Mihály, *Phys. Rev. Lett.* **52**, 149 (1984).
- [25] A. Zettle, M.B. Kaiser, and G. Grüner, *Solid State Commun.* **53**, 649 (1985).
- [26] S.E. Brown, G. Mozurkewich, and G. Grüner, *Solid State Commun.* **54**, 23 (1985); C.R. Myers and J.P. Sethna, *Phys. Rev. B* **47**, 11 194 (1993).
- [27] W. Kohn, *Phys. Rev. Lett.* **2**, 393 (1959).
- [28] J. Wong *et al.*, *Science* **301**, 1078 (2003).
- [29] R.J. McQueeney *et al.*, *Phys. Rev. Lett.* **92**, 146401 (2004).
- [30] J.C. Lashley *et al.*, *Phys. Rev. Lett.* **91**, 205901 (2003).